OncoTargets and Therapy

Dovepress
Taylor & Francis Group

Open Access Full Text Article

ORIGINAL RESEARCH

Exploration and Identification of Vitamin D and Related Genes as Potential Biomarkers for Colorectal Tumors

Lu Wang[1,2,*], Ruize Xu[2,*], Mizhu Wang[2], Menghan Wang[2], Shuai Su[1], Yuanyuan Nian[2], Xin Chen[1]

[1]Tianjin Medical University, Tianjin Medical University General Hospital, Tianjin Institute of Digestive Disease, Tian Jin, People's Republic of China; [2]Baotou Medical College, The Second Affiliated Hospital of Baotou Medical College, Baotou, People's Republic of China

*These authors contributed equally to this work

Correspondence: Xin Chen, Tianjin Medical University, Tianjin Medical University General Hospital, Tianjin Institute of Digestive Disease, Tian Jin, People's Republic of China, Email xchen03@tmu.edu.cn; Yuanyuan Nian, Baotou Medical College, the Second Affiliated Hospital of Baotou Medical College, Baotou, People's Republic of China, Email nianyuanyuannina@163.com

Objective: To explore the relationship and underlying mechanisms between vitamin D and CRC, offering valuable insights into the diagnosis and treatment of CRC.

Materials and Methods: Serum levels of $1,25(OH)_2D_3$ were measured using a double-antibody sandwich assay. Bioinformatics analysis identified vitamin D-related CRC genes, which were validated using HCT116 and HT29 cell lines. Changes in hub gene expression were analyzed via RT-qPCR.

Results: Serum levels of $1,25(OH)_2D_3$ were 42.99±6.02μg/mL in the normal group, 37.06±9.56μg/mL in the CRA group, and 19.00 ±5.96μg/mL in the CRC group ($p<0.05$). No significant differences were observed in VDR SNPs among the groups. Significant expression differences were detected in vitamin D-related colon cancer genes across the groups. LASSO regression analysis identified 5 key genes. The diagnostic model based on these genes demonstrated high diagnostic efficiency and performed well in the TCGA-COAD dataset. RT-qPCR results showed that SOSTDC1, PRKAA2, and CEACAM1 expressions decreased in the CRC and CRA groups, while MMP1 and CCND1 expressions increased. In vitro experiments indicated that calcitriol inhibits the proliferation and migration of HCT116 and HT29 cell lines and significantly alters the expression of hub genes.

Conclusion: Serum vitamin D levels are significantly lower in CRC patients. Vitamin D has been shown to inhibit the proliferation and migration of colon cancer cells and reduce the expression of oncogenes. Therefore, vitamin D holds substantial potential for the diagnosis and treatment of CRC.

Keywords: colorectal cancer, colorectal adenoma, vitamin D, vitamin D receptor, bioinformatics

Background

Colorectal cancer (CRC) is a prevalent malignant tumor of the digestive tract, ranking among the top three cancers worldwide in terms of both incidence and mortality rates.[1] Changes in lifestyle and dietary patterns have led to an increase in risk factors for CRC, contributing to its rising incidence.[2] CRC often starts insidiously and progresses rapidly, with many cases diagnosed at an advanced stage and associated with a poor prognosis, which in turn exacerbates the economic burden.[3] Most CRCs originate from colorectal adenomas (CRA), a process characterized by abnormal cellular proliferation, differentiation, evasion of apoptosis, invasion into surrounding tissues, and eventual distant metastasis. These complex processes result from interactions among genetic factors, environmental influences, and lifestyle choices.[4] Therefore, early diagnosis and prevention of CRA, the precursor lesions of CRC, are crucial for reducing both the incidence and mortality of CRC.

Vitamin D, a fat-soluble vitamin that belongs to the steroid derivative group, is absorbed through the intestine, reabsorbed by the bones, and excreted via urine. It plays a crucial role in regulating bone metabolism and maintaining calcium homeostasis,[5] which is essential for overall physiological functions and health. Research has indicated that

Received: 12 October 2024
Accepted: 7 January 2025
Published: 22 January 2025

vitamin D not only directly influences tumor cell differentiation, proliferation, and apoptosis but also indirectly affects immune cells within the tumor microenvironment,[6] showcasing its potential anti-cancer properties. The biologically active form of vitamin D, 1,25-Dihydroxyvitamin D3 (1,25(OH)2D3), binds to the nuclear vitamin D receptor (VDR), forming a complex known as vitamin D3/VDR. This complex subsequently binds to vitamin D response elements (VDREs), thereby regulating a wide range of genes and profoundly impacting various biological processess.[7,8] Studies have demonstrated that 1,25(OH)2D3 can induce the expression of anti-proliferative and pro-apoptotic genes while inhibiting oncogenic transcription factors, thereby exerting anti-cancer effects.[9] Additionally, research has found that 1,25(OH)2D3 also exhibits anti-cancer effects on CRC by binding to VDR and regulating fibroblasts in the tumor stroma.[10] VDR is a member of the nuclear receptor transcription factor superfamily and is encoded by a gene located on chromosome 12q13.11, spanning 12 exons. Research has shown that variations in the VDR gene, such as single nucleotide polymorphisms (SNPs), can influence the interaction between 1,25(OH)2D3 and VDR. Five SNPs are most commonly studied: FokI (rs2228570), BsmI (rs1544410), ApaI (rs7975232), TaqI (rs731236), and Tru9I (rs757343).[11] Despite extensive research on VDR-SNPs, findings regarding their specific impact on CRC are still inconclusive. Some studies suggest that certain VDR-SNPs may be linked to CRC in particular populations or regions. However, there is currently insufficient evidence to definitively determine the impact of VDR-SNPs on CRC development and their potential involvement in the progression from CRA to CRC.

Studying vitamin D levels and associated genes in CRC and CRA can enhance our understanding of cancer development and progression. This research aims to provide novel insights into the pathogenesis, diagnostic methods, and treatment strategies for CRC. Our objective is to examine the variations in vitamin D levels and related genes in CRA and CRC to evaluate their potential value in predicting prognosis and to develop more effective treatment strategies for CRC patients.

Methods

Samples Collection

The study included patients undergoing colonoscopies and treatments at the Digestive Endoscopy Department of the Second Affiliated Hospital of Baotou Medical College from January 2022 to December 2023. Colonoscopies and histopathological examinations were performed by the institution, with tissue samples diagnosed by the Pathology Department. Inclusion criteria included: age between 18 and 80 years, any gender, and generally good physical health. Participants must have no history of digestive system disorders, malignancies, autoimmune or metabolic diseases, as well as no cardiovascular, respiratory, endocrine, renal, hematologic, or other systemic illnesses within the past month. Exclusion criteria included: discrepancies between pathology results and endoscopic findings, recent use of vitamin D supplements, chemotherapy, participation in new drug trials, clinical diagnoses of inflammatory bowel disease, other conditions that might affect study outcomes, and inability to comply with study requirements. Within one week after the procedure, blood samples were collected in gel-containing tubes, centrifuged to separate serum from blood cells, and stored in cryovials at −80°C. Pathological specimens for RT-qPCR analysis were preserved in RNAlater solution and stored under the same conditions. This study has been approved by the Ethics Committee of the Second Affiliated Hospital of Baotou Medical College (Ethics Approval No. 2X-008), and all patients provided informed consent for endoscopic examinations and treatments.

Serum Vitamin D Detection

To measure the levels of serum $1,25(OH)_2D_3$, the double antibody sandwich method (MEIMIAN Corporation) was utilized. Initially, the frozen serum sample was allowed to equilibrate at room temperature for 60 minutes. It was then diluted five-fold and introduced into the wells of a microplate pre-coated with a capture antibody specific for human $1,25(OH)_2D_3$. Following this, HRP-labeled detection antibodies were added to facilitate the formation of antigen-antibody-enzyme complexes. The microplate was sealed and incubated at 37°C for 60 minutes. After five washes to eliminate unbound substances, TMB substrate was employed for a colorimetric reaction. The absorbance (OD value) at 450nm was measured using an ELISA reader. The content of $1,25(OH)_2D_3$ was determined based on a standard curve derived from a gradient dilution standard. All samples underwent repeated testing, and the results were analyzed to obtain mean values.

Vitamin D Receptor Gene Polymorphism Detection

Five VDR SNPs (FokI rs2228570, BsmI rs1544410, ApaI rs7975232, TaqI rs731236, and Tru9I rs757343) were detected using the Snapshot method. Genomic DNA was extracted from blood samples using a silicon-based adsorption column (Cat. D0063, Biyuntian Biotechnology). The PCR reaction was carried out in a total volume of 15 μL, comprising 1 μL of DNA, 1.5 μL of 10x Buffer, 0.3 μL of dNTPs (10 mmol), 1.5 μL of MgCl2 (25 mmol), 0.15 μL of each primer (10 μmol), 0.3 μL of Taq enzyme (5 U/μL), and sterile water to make up the volume. The PCR protocol included an initial denaturation step at 94°C for 3 minutes, followed by 30 cycles of denaturation at 94°C for 15 seconds, annealing at 55°C for 15 seconds, and extension at 72°C for 30 seconds, with a final extension at 72°C for 3 minutes. PCR products were subsequently analyzed using 3% agarose gel electrophoresis. For purification, ExoI and FastAP enzymes were used, followed by an extension reaction with pre-mixed primers. Each extension reaction had a volume of 6 μL, containing 2 μL of PCR product, 1 μL of Snapshot Mix reagent, and sterile water. The extension conditions were 1 minute at 96°C, followed by 30 cycles of 10 seconds at 96°C, 5 seconds at 52°C, and 30 seconds at 60°C. Sequencing was performed using a 3730XL Genetic Analyzer after denaturation and cooling in Hi-Di™ formamide. The locations and primers of VDR SNP are in Table 1.

Bioinformatics Analysis

Dataset Retrieval

We retrieved mRNA sequencing data for normal colon mucosa (NC), CRA, and CRC from the GSE20916 and GSE37364 datasets in the GEO database. Prognostic analysis data for CRC were sourced from the TCGA-COAD project available on the TCGA portal website (https://portal.gdc.cancer.gov).[12] Additionally, for in-depth research, we extracted gene information related to "vitamin D" and "vitamin D receptor" from the Molecular Signature Database (MsigDB) (http://www.gsea-msigdb.org/gsea/msigdb/). After screening and removing duplicates from previous GSEA MsigDB studies, we successfully assembled a list of 299 unique genes related to vitamin D.

Differential Genes Analysis

We analyzed the GSE20916 and GSE37364 datasets using GEO2R (https://www.ncbi.nlm.nih.gov/geo/geo2r/) to identify differentially expressed genes (DEGs) between normal mucosa and CRA, as well as between normal mucosa and CRC. We used $|\log FC| > 1$ and $p < 0.05$ as criteria for differential expression. The data from different groups were visualized, and volcano maps were generated using the Sangerbox online tools (http://www.sangerbox.com/tool).[13]

Enrichment Analysis

Gene Ontology (GO) annotation was performed using the org.Hs.eg.db package (version 3.1.0), and gene annotations for KEGG pathways were obtained via the KEGG REST API (https://www.kegg.jp/kegg/rest/keggapi.html). These annotations served as the background for mapping genes to the corresponding background set. Enrichment analysis was conducted using the R packages clusterProfiler (version 4.4.4) and GOplot (version 1.0.2) to identify significantly enriched gene sets. The GO enrichment analysis covered terms such as biological process (BP), molecular function

Table 1 Locations and Primers of VDR SNP

Locations	Primers	Length and GC Content of PCR	Polymorphism
FokI (rs2228570)	F:AAGCTGAAACTGGATCCCTTC R:TGCTGTGCAGAAGCTCTTTAG	232;37.5%	G/C (1:0)
BsmI (rs1544410)	F:TGTCCCCAAGGTCACAATAAC R:TGAAGGGAGACGTAGCAAAAG	428;51.9%	C/T (0.944:0.056)
Tru9I (rs757343)	F:TGTCCCCAAGGTCACAATAAC R:TGAAGGGAGACGTAGCAAAAG	428;51.9%	C/T (0.793:0.207)
ApaI (rs7975232)	F:ATGTACGTCTGCAGTGTGTTG R:TATCACCGGTCAGCAGTCATAG	217;62.2%	C/A (0687:0.313)
TaqI (rs731236)	F:ATGTACGTCTGCAGTGTGTTG R:TATCACCGGTCAGCAGTCATAG	217;62.2%	A/G (0.95:0.05)

https://doi.org/10.2147/OTT.S495066

(MF), and cellular component (CC). A minimum gene set size of 5 and a maximum of 5000 were set, with statistical significance determined by a p-value < 0.05 and a false discovery rate (FDR) < 0.25. Visualization of the results was conducted using the R package ggplot2 (version 3.3.6).

LASSO Regression Analysis

The LASSO regression analysis was applied to construct diagnostic features. The "glmnet" package in R was employed for cross-gene regression analysis to identify key feature genes associated with CRC in two datasets. The cleaned data was analyzed using the "glmnet" package to obtain lambda values, likelihood values, and classification error rates for the variables. The results were then visualized to illustrate the findings.

Immune Infiltration Analysis

Using the "CIBERSORT" algorithm combined with the LM22 reference set, we deconvolved the cellular composition of tissues based on gene expression data. Immune infiltration analysis was performed on the GSE20916 and GSE37364 datasets using CIBERSORTx (https://cibersortx.stanford.edu/). Following this, heat map analysis was performed to visualize the expression of hub genes and the 22 types of immune cells.

RT-qPCR

To confirm the expression of hub genes, RT-qPCR experiments were performed with the following steps: Total RNA was first extracted using the Trizol reagent and then purified with the RNeasy kit. The total mRNA was reverse transcribed into cDNA using a reverse transcription kit under the conditions of incubation at 25°C for 10 minutes, at 55°C for 30 minutes, at 85°C for 5 minutes, and then cooled to 4°C. In three independent experiments, specific qPCR primers were used to amplify the genes SOSTDC1, PRKAA2, CEACAM1, MMP1, CCND1, and GAPDH in triplicate (Table 2). The data were analyzed using the ΔΔCt method.

Immunohistochemistry (IHC)

The IHC validation of hub genes includes two parts: clinical colon tissue IHC and the HPA database. The HPA database (https://www.proteinatlas.org/) validated genes such as PRKAA2, CEACAM1, and CCND1. Genes validated through IHC in clinical tissues include SOSTDC1 and MMP1. The specific IHC procedure includes the following steps: Tissue was fixed in formalin and embedded in paraffin, then sliced into 4 μm thick sections. The sections were then baked, deparaffinized, and hydrated. Blocking was performed using 5% goat serum for 30 minutes, followed by incubation with primary antibodies targeting SOSTDC1 and MMP1 (purchased from Youpin Biotechnology, China) overnight at 4°C. Afterward, the sections were incubated with a secondary antibody at 37°C for 30 minutes. After PBS washing, the sections were subjected to diaminobenzidine (DAB) staining, hematoxylin counterstaining, dehydration, and mounted with neutral gum for microscopic examination.

Table 2 Primers for RT-qPCR

Name	Primer Sequences (5′-3′)	Length
hGAPDH-F	GGAGCGAGATCCCTCCAAAAT	197
hGAPDH-R	GGCTGTTGTCATACTTCTCATGG	
h-SOSTDC1-F	ACCCGTACCCAGAGAATCCA	79
h-SOSTDC1-R	TGCAGGCAGTGACTACTGTG	
h-PRKAA2-F	CGGGTGAAGATCGGACACTA	105
h-PRKAA2-R	AACTGCCACTTTATGGCCTG	
h-CEACAM1-F	AAAATGGCCTCTCACCTGGG	134
h-CEACAM1-R	GGGTCATTGGAGTGGTCCTG	
h-MMP1-F	AGAAAGAAGACAAAGGCAAGTTGA	169
h-MMP1-R	AAACTGAGCCACATCAGGCA	
h-CCND1-F	GAGGCGGAGGAGAACAAACA	96
h-CCND1-R	GGAGGGCGGATTGGAAATGA	

Cell Culture

Human colon cancer cells HCT116 and HT29 were purchased from Wuhan Punuo Sai Life Technology Co., Ltd. We customized specific culture media based on experimental requirements and cultured these two cell types in the respective media. The cells were maintained in a humidified incubator with 5% CO2 at a constant temperature of 37°C. For experiments involving calcitriol concentration screening, the cells were treated with calcitriol at designated time points.

Cell Proliferation and Migration Assays

Cells treated with calcitriol were plated in 96-well plates. For the proliferation assay, 10 μL of CCK-8 solution was added to each well and incubated at 37°C for 2 hours. The optical density was measured using an iMark microplate reader (Bio-Rad) at a wavelength of 450 nm. The cell inhibition rate (%) was calculated using the formula [(Ac-As)/(Ac-Ab)]×100, where As denotes the absorbance of the experimental wells containing cells, culture medium, CCK-8, and drugs; Ab represents the absorbance of the blank wells containing only culture medium and CCK-8; and Ac indicates the absorbance of the control wells containing cells, culture medium, and CCK-8. To evaluate cell migration ability, scratch assays were performed in 6-well plates. Images of initial scratches (0 hour) and subsequent observations (24 hours) were analyzed using ImageJ software to measure changes in the scratched area.

Statistical Analysis

All experimental results are presented as mean ± standard deviation (SD). Differences in vitamin D levels among the groups were evaluated using one-way analysis of variance (ANOVA). The Spearman correlation analysis was employed to assess the relationships between central genes and immune cells. A P value < 0.05 was considered statistically significant, with * denoting $P < 0.05$, ** denoting $P < 0.01$, and *** denoting $P < 0.001$. All bioinformatics analyses were conducted using R software (version 4.2.1) and Sangerbox online tools.

Results

Vitamin D Concentration

According to the inclusion and exclusion criteria, a total of 80 cases were enrolled: 20 cases without intestinal abnormalities (control group), 40 cases with CRA, and 20 cases with CRC. The serum levels of $1,25(OH)_2D_3$ ranged from 10.00 to 56.35 μg/mL, with an average value of (34.02±12.02 μg/mL). *t*-test analysis revealed no significant differences in $1,25(OH)_2D_3$ levels based on gender ($t=1.752$, $p=0.084$) or age ($t=0.91$, $p=0.432$). However, the Mann–Whitney *U*-test revealed significant differences in $1,25(OH)_2D_3$ levels among the groups: the control group (42.99±6.02 μg/mL), the CRA group (37.06±9.56 μg/mL), and the CRC group (19.00±5.96 μg/mL) ($p<0.05$) (Figure 1A).

VDR Gene Polymorphisms in Different Groups

According to the reference,[11] five VDR SNP loci associated with CRC were selected and analyzed in blood cell samples from 80 patients. For the FokI (rs2228570) gene, the allele frequencies for "G" and "C" were 99.40% and 0.60%, respectively. The "GG" homozygous genotype was present in both the CRC and CRA groups, while the control group exhibited only one case (3%) of the "GC" heterozygous genotype. The "CC" genotype was not detected in any of the groups. No statistically significant differences were observed in allele frequencies or genotype distributions between the groups.

For the BsmI (rs1544410) gene, the allele frequencies for "C" and "T" were 93.10% and 6.90%, respectively. In the CRC, CRA, and control groups, the frequency of the "CC" homozygous genotype was 90%, 82.5%, and 90%, respectively. The frequencies of the "CT" heterozygous genotype were 10%, 17.5%, and 10%, respectively, with no instances of the "TT" genotype detected. Statistical analysis indicates that there are no significant differences in allele frequencies or genotype distributions among the groups. For the Tru9I (rs757343) gene, the allele frequencies for "C" and "T" were 83.80% and 16.30%, respectively. In the CRC, CRA, and control groups, the frequency of the "CC" homozygous genotype was 70% in each group. The "CT" heterozygous genotype frequencies were 25% in the CRC group, 25% in the control group, and 30% in the control group. The "TT" genotype was observed at a frequency of 5% in CRC and control groups but was not detected in the CRA group. Statistical analysis revealed no significant differences in

https://doi.org/10.2147/OTT.S495066

https://doi.org/10.2147/OTT.S495066

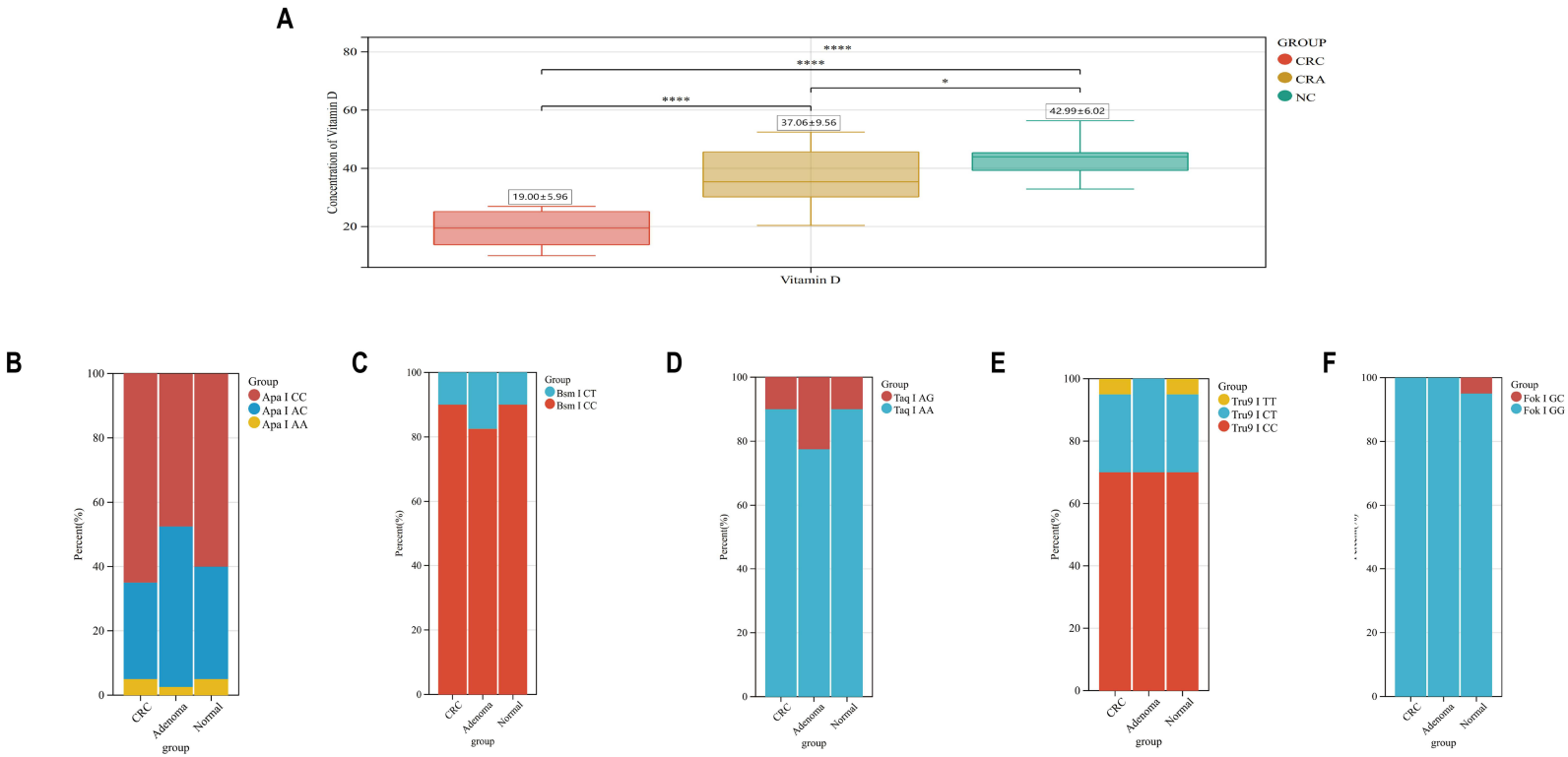

Figure 1 (**A**) Box plot of vitamin D concentrations across different groups; (**B–F**) Cumulative bar chart of VDR SNP across different groups. (* p< 0.05, ** p< 0.01, *** p< 0.001, **** p < 0.0001).

Table 3 Distribution of Allele Frequencies of VDR SNP Polymorphisms in Different Groups

	Fok I		Bsm I		Tru9 I		Apa I		Taq I	
	G	C	C	T	C	T	A	C	A	G
Total	159	1	149	11	134	26	39	121	147	13
	99.40%	0.60%	93.10%	6.90%	83.80%	16.30%	24.40%	75.60%	91.90%	8.10%
CRC	40	0	38	2	33	7	8	32	38	2
	100%	0.00%	95%	5%	82.50%	17.50%	20.00%	80.00%	95.00%	5.00%
CRA	80	0	73	7	68	12	22	58	71	9
	100%	0.00%	91.30%	8.70%	85.00%	15.00%	27.50%	72.50%	88.80%	11.20%
Control	39	1	38	2	33	7	9	31	38	2
	97.50%	2.5%	95%	5%	82.50%	17.50%	22.50%	77.50%	95.00%	5.00%
X^2	3.019		0.879		0.184		0.915		2.093	
P	0.221		0.644		0.912		0.633		0.351	

Table 4 Distribution of Genotype Frequencies of VDR SNP Polymorphisms in Different Groups

	Fok I		Bsm I		Tru9 I			Apa I			Taq I	
	GG	GC	CC	CT	CC	CT	TT	AA	AC	CC	AA	AG
Total	79	1	69	11	56	22	2	3	33	44	67	13
	98.80%	1.30%	86.30%	13.80%	70.00%	27.50%	2.50%	3.80%	41.30%	55.00%	83.80%	16.30%
CRC	20	0	18	2	14	5	1	1	6	13	18	2
	100.00%	0.00%	90%	10%	70.00%	25.00%	5.00%	5.00%	30.00%	65.00%	90.00%	10.00%
CRA	40	0	33	7	28	12	0	1	20	19	31	9
	100.00%	0.00%	82.50%	17.50%	70.00%	30.00%	0.00%	2.50%	50.00%	47.50%	77.50%	22.50%
Control	19	1	18	2	14	5	1	1	7	12	18	2
	95%	5%	90%	10%	70.00%	25.00%	5.00%	5.00%	35.00%	60.00%	90.00%	10.00%
X^2	3.038		0.949		2.182			2.742			2.296	
P	0.219		0.622		0.702			0.602			0.317	

allele frequencies or genotype distributions among the groups. For the ApaI (rs7975232) gene, the allele frequencies or "A" and "C" were 24.40% and 75.60%, respectively. In the CRC, CRA, and control groups, the frequency of the "AA" homozygous genotype was 5%, 2.5%, and 5%, respectively. The "CC" homozygous genotype frequencies were 65% in the CRC group, 47.5% in the CRA group, and 60% in the control group, while the "AC" heterozygous genotype frequencies were 30%, 50%, and 35.5%, respectively. Statistical analysis indicates that there are no significant differences in allele frequencies or genotype distributions among the groups. For the TaqI (rs731236) gene, the allele frequencies for "A" and "G" were 91.90% and 8.10%, respectively. In the CRC, CRA, and control groups, the frequency of the "AA" homozygous genotype was 90%, 77.5%, and 90%, respectively. The "AG" heterozygous genotype frequencies were 10% in the CRC group, 22.5% in the CRA group, and 10% in the control group. The "GG" genotype was not detected in any of the samples. Statistical analysis revealed no significant differences in allele frequencies or genotype distributions among the groups (Tables 3 and 4) (Figure 1B–F).

Bioinformatics Analysis

Screening of Differential Genes

Two GEO datasets, GSE20916 and GSE37364, were selected for differential expression analysis of normal intestinal mucosa, CRA, and CRC. In the GSE20916 dataset, a total of 2817 genes were differentially expressed between normal mucosa and CRA, with 1375 genes upregulated and 1442 genes downregulated. Between normal mucosa and CRC, there were 3795 differentially expressed genes, with 1923 genes upregulated and 1872 genes downregulated. In the GSE37364

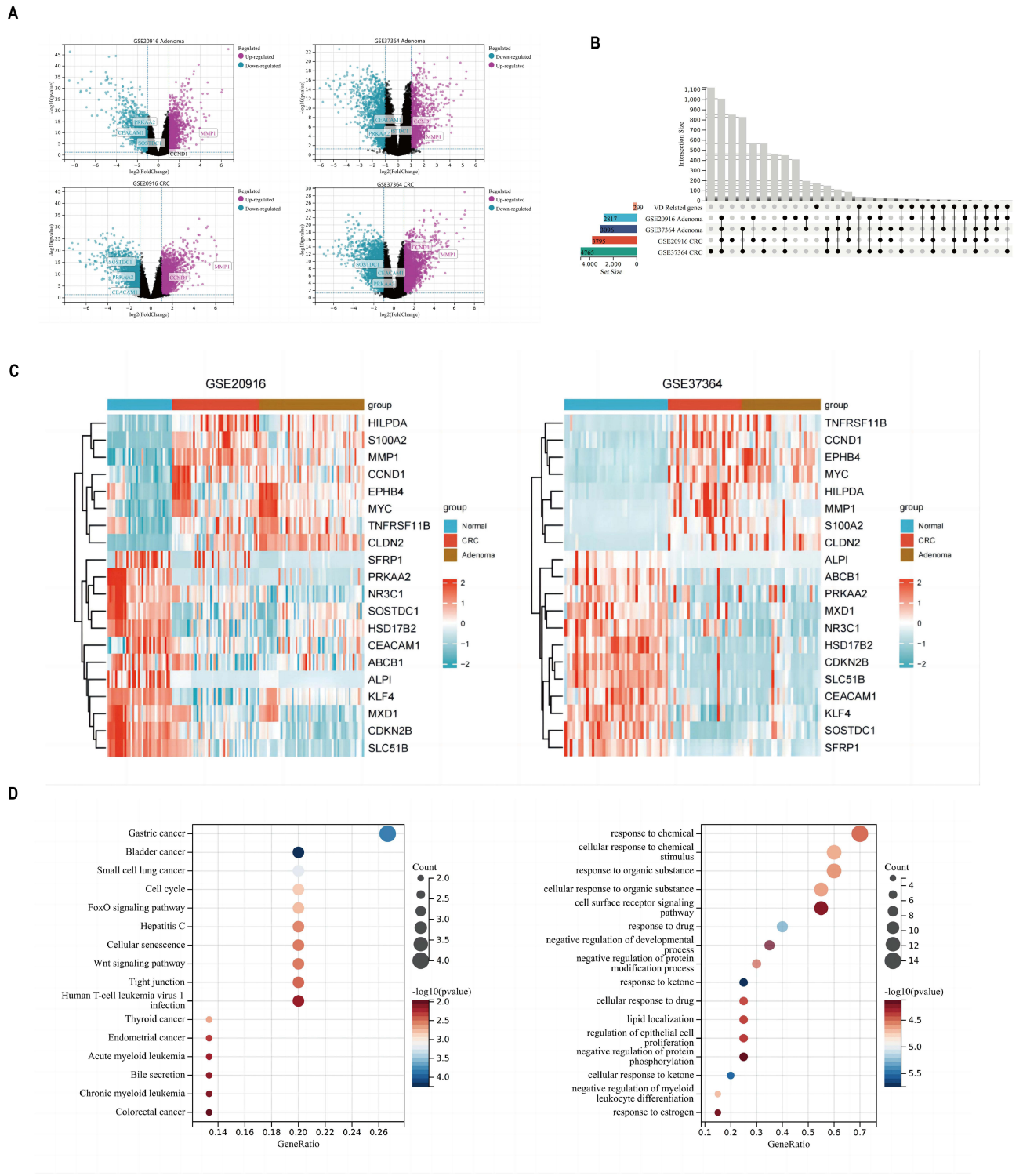

Figure 2 Volcano plot,UpSet plot and enrichment results. (**A**) Volcano plot for DEGs between normal, CRA, and CRC in the GSE20916 and GSE37364 datasets. (**B**) UpSet plot for the intersection of DEGs and vitamin D-related genes. (**C**)The heatmaps of VDDEGs in the GSE20916 and GSE37364 datasets. (**D**) GO and KEGG enrichment results of VDDEGs.

dataset, a total of 3096 genes were differentially expressed between normal mucosa and CRA, including 1168 upregulated and 1968 downregulated genes. Between normal mucosa and CRC, there were 4765 differentially expressed genes, with 2391 upregulated and 2374 downregulated (Figure 2A).

Across two datasets, common DEGs were identified as vitamin D-related colorectal tumor genes (VDDEGs), totaling 20 genes including MMP1, CCND1, PRKAA2, S100A2, and CLDN2 (Figure 2B). Heatmaps were utilized to further investigate the expression patterns of these genes, revealing significant differences among normal mucosa, CRA, and CRC groups. A cohesive trend emerged, indicating a progression from CRA to CRC (Figure 2C).

Enrichment Analysis

GO and KEGG enrichment analyses were performed based on VDDEGs to elucidate the molecular functions of these overlapping genes (Figure 2D). The GO analysis identified key terms such as response to ketones, cellular response to ketones, response to drugs, negative regulation of myeloid leukocyte differentiation, and cellular response to chemical stimuli. The KEGG analysis highlighted primary pathways including bladder cancer, gastric cancer, small cell lung cancer, cell cycle, and CRC.

LASSO Analysis

Using LASSO regression analysis on the GSE20916 dataset (Figure 3A and B), the optimal λ value for CRC diagnosis was determined to be 0.0054. This analysis identified nine variables with non-zero coefficients: SOSTDC1, HILPDA, MYC, CCND1, S100A2, CEACAM1, CLDN2, MMP1, and PRKAA2. For the GSE37364 dataset, the optimal λ value was 0.01789, identifying ten variables with non-zero coefficients: SOSTDC1, HSD17B2, TNFRSF11B, CCND1,

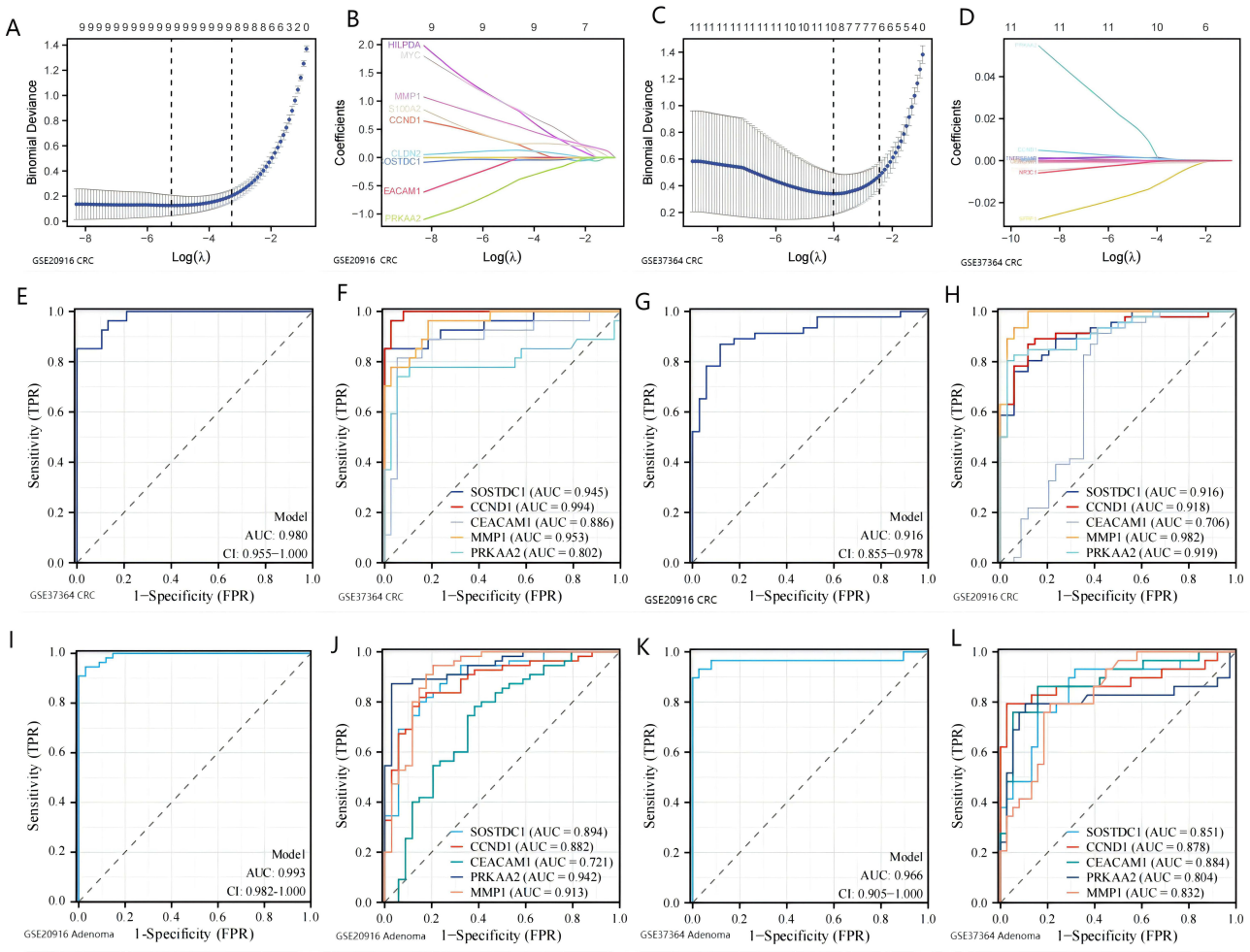

Figure 3 LASSO analysis and ROC curves. (**A**) LASSO regression coefficients in the GSE20916 dataset. (**B**) Variables with nine non-zero regression coefficients identified by LASSO analysis in the GSE20916 dataset. (**C**) LASSO regression coefficients in the GSE37364 dataset. (**D**) Variables with ten non-zero regression coefficients identified by LASSO analysis in the GSE37364 dataset. (**E–H**) ROC curves for CRC groups in the GSE20916 and GSE37364 datasets. (**I–L**) ROC curves for CRA groups in the GSE20916 and GSE37364 datasets.

https://doi.org/10.2147/OTT.S495066

CEACAM1, SFRP1, SLC51B, MMP1, PRKAA2, and NR3C1) (Figure 3C and D). Cross-LASSO analysis showed five common genes across both datasets: SOSTDC1, CCND1, CEACAM1, MMP1, and PRKAA2. These hub vitamin D-related genes in CRC served as the foundation for the diagnostic model.

The models evaluated in two datasets demonstrated robust predictive capabilities (AUC > 0.8) across both the CRA and CRC groups through ROC curve analysis. The diagnostic model built on these five hub genes exhibited excellent performance, with AUC values exceeding 0.9, in both the CRA and CRC groups (Figure 3E–L).

Immune Infiltration

Immune cell infiltration analysis was performed on the GSE20916 and GSE37364 datasets using CIBERSORT (Figure 4). The box plots illustrate consistent trends of immune cell infiltration across normal colon mucosa, CRA, and CRC groups. The

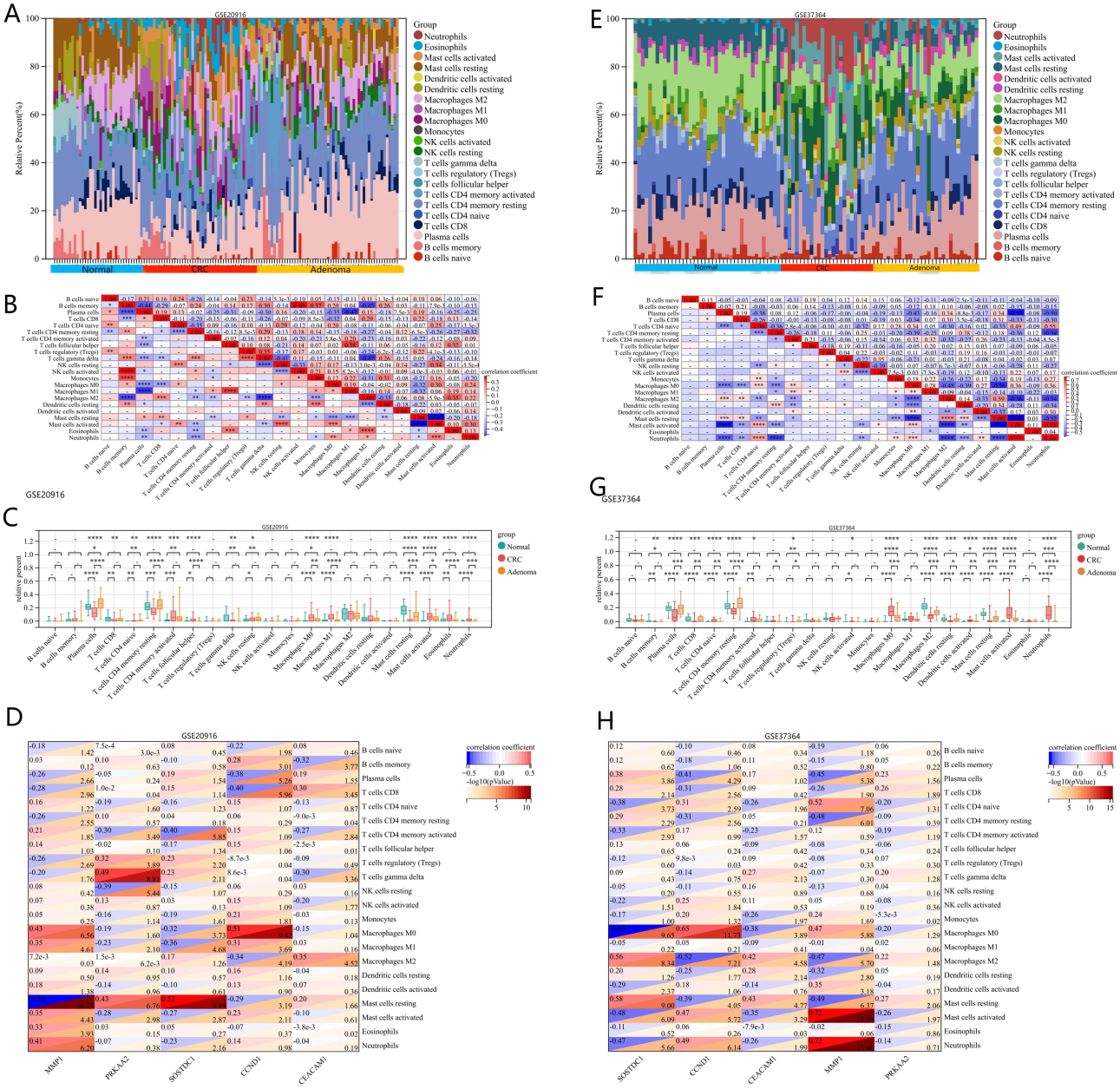

Figure 4 Immune infiltration analysis. (**A**) Immune infiltration bar plot of the GSE20916 dataset. (**B**) Heatmap of immune cell correlation in the GSE20916 dataset. (**C**) Distribution and comparison of immune cells in the normal control group, Adenoma group, and CRC group in the GSE20916 dataset. (**D**) Heatmap of the correlation between key genes and immune cells in the GSE20916 dataset. (**E**) Immune infiltration bar plot of the GSE37364 dataset. (**F**) Heatmap of immune cell correlation in the GSE37364 dataset. (**G**) Distribution and comparison of immune cells in the normal control group, CRA group, and CRC group in the GSE37364 dataset. (**H**) Heatmap of the correlation between key genes and immune cells in the GSE37364 dataset. (* p< 0.05, ** p< 0.01, *** p< 0.001, **** p < 0.0001).

https://doi.org/10.2147/OTT.S495066

analysis highlighted significant differences in the levels of T cells, dendritic cells, macrophages, and mast cells among these groups in the colon. In CRC, there was a notable increase in activated mast cells, M1 macrophages, and neutrophils, with similar increases observed in the CRA group compared to normal mucosa. These findings suggest that abnormal immune cell infiltration progressively intensifies during the development of colon tumors.

A heatmap illustrating the correlation between immune infiltrating cells and hub genes reveals the following relationships: MMP1 is positively correlated with M0 macrophages and neutrophils, but negatively linked to M1 macrophages and resting mast cells. PRKAA2 shows a positive relationship with T cells and resting mast cells, while SOSTDC1 exhibits a significant positive correlation with resting mast cells. CCND1 is notably positively correlated with M0 macrophages, whereas CEACAM1 is positively correlated with M2 macrophages and mast cells. In the TCGA-COAD database, analysis of immune infiltration associated with these hub genes suggests their role in mediating immune responses throughout colon tumor progression.

Expression and Validation of Hub Genes

In the GSE37364 dataset, the refined sample groups include normal colon mucosa, CRA, CRC Dukes A/B phase, and CRC Dukes C/D phase. Comparative analysis of gene expression across these groups (Figure 5A) reveals that as disease severity progresses, the expression levels of SOSTDC1, PRKAA2, and CEACAM1 gradually decrease, while MMP1 and CCND1 exhibit a progressive increase in expression levels. These findings suggest that hub genes play a crucial role in the progression from colon adenomas to cancer.

The analysis of TCGA-COAD sequencing data (including both paired and unpaired samples) revealed significant differences in hub gene expression between the normal control group and the CRC group (Figure 5B and C), aligning with our research dataset. In the TCGA-COAD data, these hub genes exhibited strong diagnostic performance, with AUC values exceeding 0.8 for each gene (Figure 5D).

RT-qPCR Results of the Hub Genes

RT-qPCR analysis was conducted on five randomly selected patients from each group to validate the expression trends of hub genes observed in the GEO and TCGA databases. The results confirmed that the expression levels of SOSTDC1, PRKAA2, and CEACAM1 gradually decreased with increasing disease severity, while MMP1 and CCND1 exhibited a progressive increase. Statistically significant differences were observed between the groups (Figure 5E).

IHC Results of the Hub Genes

The expression changes of PRKAA2, CEACAM1, and CCND1 proteins were analyzed through the HPA database. The results showed that CCND1 expression was significantly higher in CRC tissues compared to normal colorectal tissues, while PRKAA2 and CEACAM1 expression were lower in CRC tissues than in normal colorectal tissues. Additionally, the protein expression of SOSTDC1 and MMP1 was analyzed and validated through clinical tissue IHC. The results indicated that MMP1 expression was significantly higher in CRC tissues than in normal colorectal tissues, whereas SOSTDC1 expression was lower in CRC tissues compared to normal colorectal tissues(Figure 5F). These results were consistent with the trends observed in the RT-qPCR data from clinical tissues.

Cell Experiments

After stimulating HT29 cells with calcitriol at varying concentrations, the effects on colorectal cancer cell proliferation and migration were assessed using the CCK-8 proliferation assay and the scratch assay. The results demonstrated that calcitriol inhibited both proliferation and migration in a dose-dependent manner, with more pronounced effects at higher concentrations (Figure 6A–C).

RT-qPCR analysis of HCT116 and HT29 cell lines treated with 100nM calcitriol revealed a significant upregulation of SOSTDC1, PRKAA2, and CEACAM1, while MMP1 and CCND1 expression was significantly downregulated (Figure 6D). The regulatory trends of MMP1, PRKAA2, and SOSTDC1 in these two cell lines were consistent, indicating a statistically significant difference after intervention.

https://doi.org/10.2147/OTT.S495066

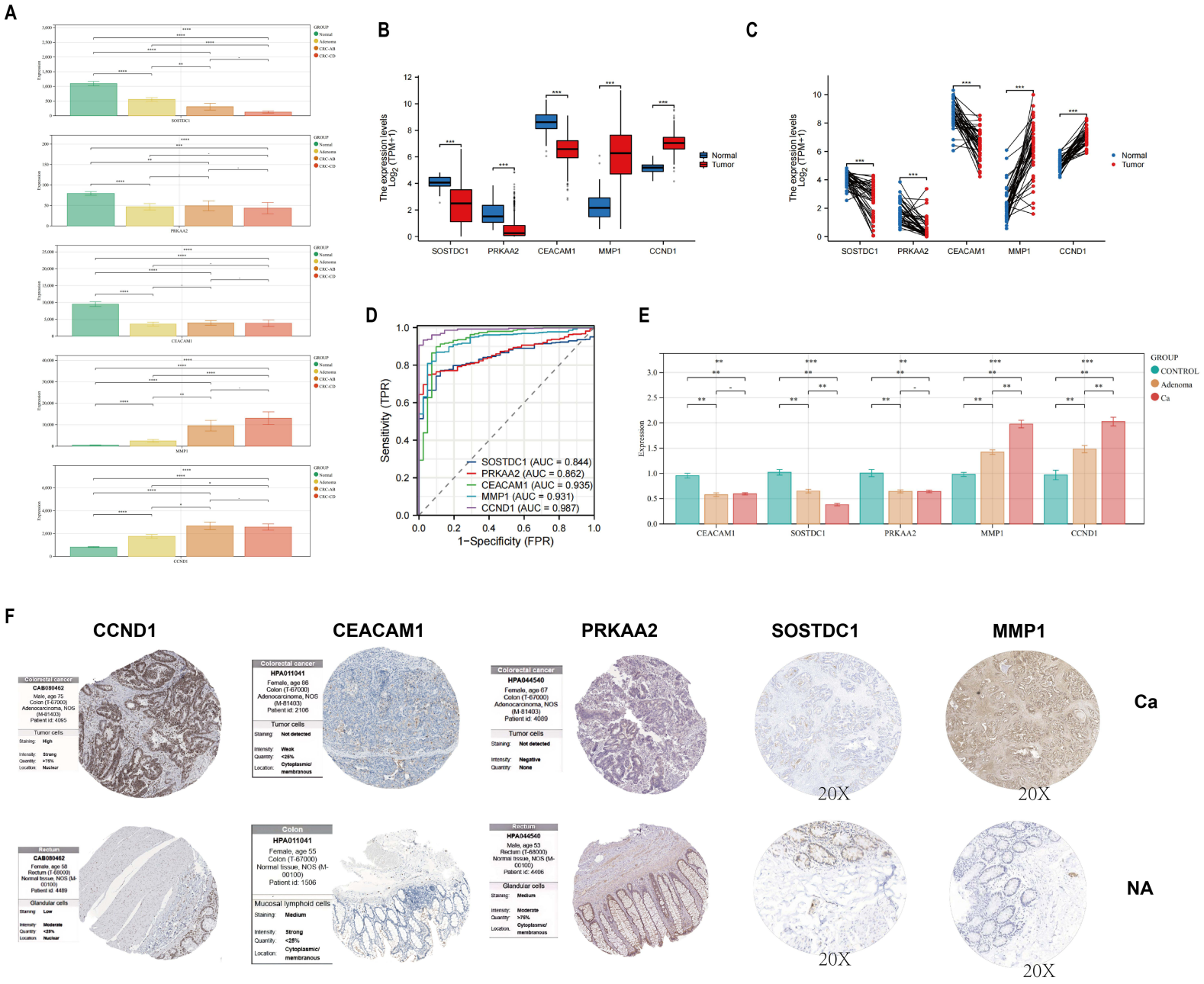

Figure 5 Expression and verification of hub genes. (**A**) Expression of hub genes across four groups in the GSE37364 dataset. (**B** and **C**) Expression of hub genes in TCGA-COAD dataset. (**D**) ROC curves of hub genes based on expression profiles from TCGA-COAD dataset. (**E**) RT-qPCR results of hub genes. (**F**) IHC results of hub genes. (* p< 0.05, ** p< 0.01, *** p< 0.001, **** p < 0.0001).

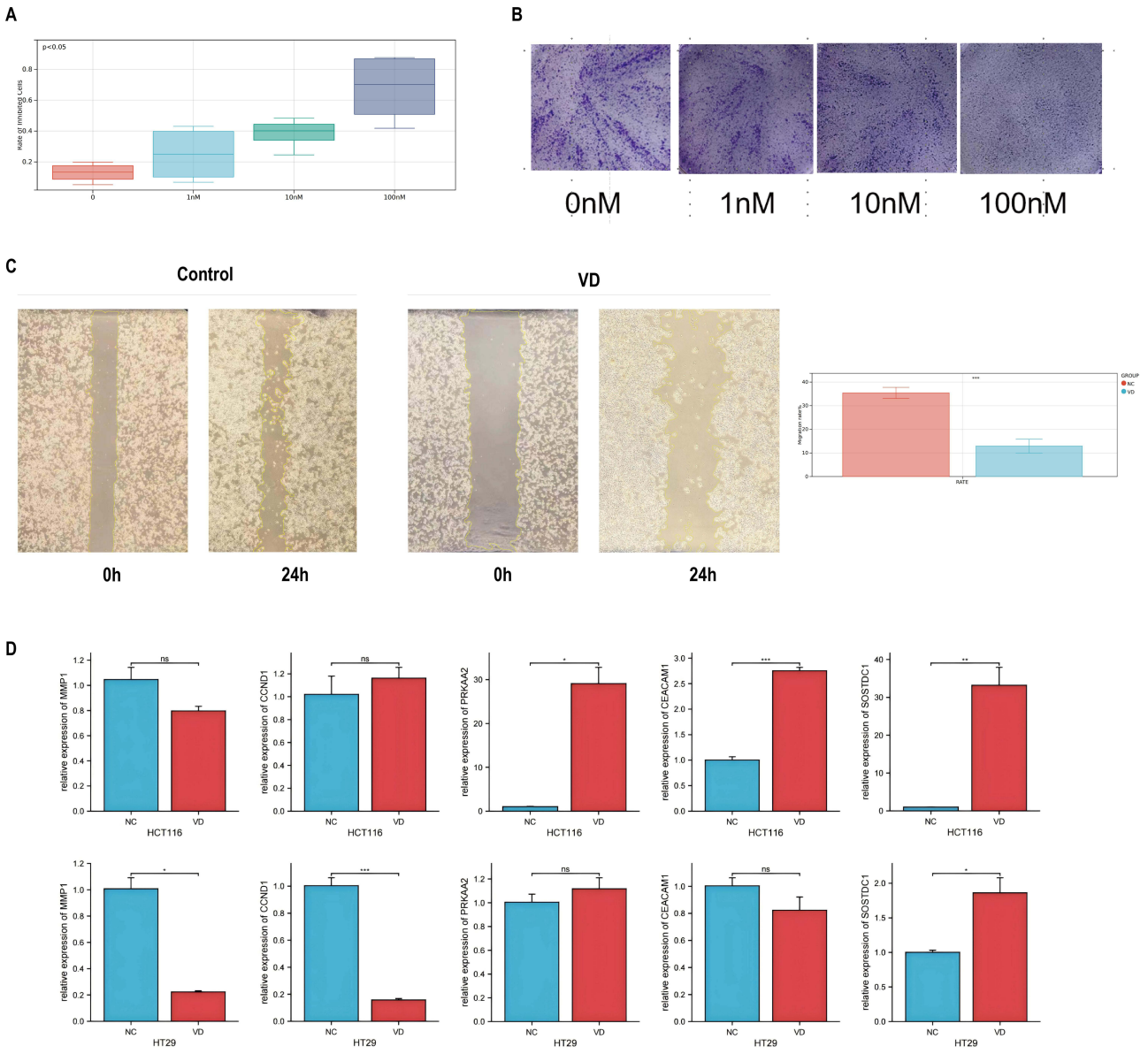

Figure 6 Effects of calcitriol on CRC cells. (**A**) Column chart of CCK-8 assay results after intervention with different concentrations of calcitriol in HT29 cells. (**B**) Plate clone assay results after intervention with the same concentration of calcitriol in HT29 cells. (**C**) Scratch assay results at 24 hours after treatment with 10^2nM calcitriol in HT29 cells. (**D**) Column chart of RT-qPCR results after treatment with 10^2nM calcitriol in HCT116 and HT29 cell lines. (* p< 0.05, ** p< 0.01, *** p< 0.001, **** p < 0.0001).

Discussion

CRC presents a significant global health challenge due to its high incidence and mortality rates. Although advances in surgical and chemotherapy techniques have improved patient outcomes through tumor resection and effective treatment, late-stage diagnosis is often associated with high mortality and poor prognosis. CRA, a critical precancerous lesion, is essential for the prevention and management of CRC. Early detection and prompt treatment of adenomas are vital for reducing both the incidence and mortality rates of CRC.

Epidemiological data indicate that vitamin D deficiency is linked to increased incidence or mortality rates of CRC.[14] Studies suggest that vitamin D has anti-tumor effects by influencing tumor cell differentiation, proliferation, and apoptosis, as well as by modulating both innate and adaptive immunity within the tumor microenvironment.[15] Our study found that CRC and CRA patients have lower serum levels of $1,25(OH)_2D_3$ in compared to healthy individuals, consistent with prior studies.[16] However, while $1,25(OH)_2D_3$ levels were reduced in CRA patients, the decrease reduction was not as pronounced as in CRC patients. This suggests that as adenomas advance to cancer, the production

https://doi.org/10.2147/OTT.S495066

or utilization of $1,25(OH)_2D_3$ may be influenced, highlighting its crucial role in disease progression. Although cancer and polyp incidence are age-related, we did not observe significant differences in serum $1,25(OH)_2D_3$ levels across various age groups. Therefore, vitamin D deficiency appears to be more closely associated with the progression of CRA and CRC rather than being solely attributable to age-related factors.

Vitamin D exerts anti-tumor effects by binding to the VDR. Upon heterodimerization with the retinoid X receptor (RXR) in the nucleus, this complex binds to the vitamin D response elements (VDREs) in the promoter region of target genes, thereby activating transcription.[17,18] Consequently, variations or deficiencies in VDR may lead to symptoms associated with vitamin D deficiency. SNPs in the VDR gene are closely linked to various cancers.[19] For instance, a study involving 256 Saudis found that SNPs such as TaqI and ApaI increase the risk of CRC, while the BsmI SNP appears to have a protective effect.[20] Another study involving 69 Chinese CRC patients and 218 healthy individuals suggested that the FokI SNP polymorphism might reduce the risk of CRC.[21] We investigated the association between VDR SNPs and the progression of CRA and CRC. The absence of the recessive allele "C" of FokI in both CRC and CRA patients suggest a potential protective effect against cancer. Additionally, compared to the CRC and normal control groups, the frequency of the TaqI homozygous dominant genotype "AA" was lower in the CRA group, which could be related to the early onset of CRC. However, these alleles or genotypes did not show statistically significant differences among the three groups, indicating that further validation of our hypotheses is needed.

We utilized bioinformatics methods to analyze microarray datasets with the goal of identifying prognostic markers in NC-CRA-CRC. To further investigate the molecular mechanisms of vitamin D, we analyzed transcriptomic data from public databases, focusing on key candidate genes such as SOSTDC1, CCND1, CEACAM1, MMP1, and PRKAA2. By using CIBERSORT to analyze immune cell infiltration in the GS20916 and GSE37364 datasets, we revealed variations in cell abundance in colon mucosa, CRA, and CRC. These findings suggest that genes like SOSTDC1, CCND1, CEACAM1, MMP1, and PRKAA2 may serve as potential biomarkers for the early diagnosis of CRC and CRA monitoring.

According to the MsigDB database, MMP1 and PRKAA2 are associated with abnormal vitamin D metabolism. MMP1 (matrix metalloproteinase-1) is crucial for the remodeling of the extracellular matrix in colorectal cancer cells, and its dysregulation can affect cancer invasion, metastasis, and prognosis.[22] Studies indicate that serum vitamin D levels in patients with knee osteoarthritis are negatively correlated with MMP1 expression, suggesting that vitamin D deficiency may increase MMP1 activity by inhibiting interleukin-1β.[23,24] PRKAA2 (protein kinase AMP-activated catalytic subunit alpha 2) encodes the α 2 subunit of AMPK, which regulates cellular energy and metabolic processes such as glucose and fatty acid metabolism, protein synthesis, and cell proliferation. AMPK activation helps maintain energy balance by promoting catabolic pathways and inhibiting cell growth, thus impacting tumorigenesis.[25] Additionally, PRKAA2 influences the PI3K-AKT-mTOR signaling pathway in tumor cells through vitamin D3, participating in oxidative stress processes and affecting cell survival and infiltration.[26]

SOSTDC1, CCND1, and CEACAM1 interact with the vitamin D receptor. SOSTDC1 (sclerostin domain-containing protein 1) is encoded by the SOST gene and is mainly expressed in bone, kidney, and pancreatic tissues, participating in the regulation of bone metabolism, kidney development, and insulin secretion.[27] SOSTDC1 works by regulating BMP and Wnt signaling pathways associated with disease pathogenesis, including cancer.[28–31] Its specific role in CRC still needs further research. CCND1 (cyclin D1) encodes cyclin D1, a key protein that interacts with CDKs during the transition from G1 to S phase, and is responsible for regulating the progression of the cell cycle.[32] Due to cell cycle dysregulation, overexpression of CCND1 is linked to the occurrence of various cancers, including CRC.[33–35] CEACAM1 (carcinoembryonic antigen-related cell adhesion molecule 1) is a cell adhesion molecule that is widely expressed in epithelial cells, leukocytes, and tumor cells. It plays a crucial role in regulating intercellular adhesion, signal transduction, cell proliferation, apoptosis, and immune response.[36] Reduced expression of CEACAM1 may impair intercellular adhesion, promoting tumor invasion and metastasis, and influencing the tumor microenvironment and immune evasion. In cancer patients, lower levels of CEACAM1 are correlated with malignancy, lymph node metastasis, and poor prognosis.[37–39] However, the specific mechanisms of CEACAM1 in CRC still need further investigation.

This study compared crossover genes between CRA and CRC, validating the findings with qPCR in clinical samples. It discovered that vitamin D-related genes (CEACAM1, SOSTDC1, and PRKAA2) are reduced in both CRA and CRC, suggesting their protective roles in the progression from mucosa to CRA to CRC. Conversely, MMP1 and CCND1 are elevated, which may promote disease progression. The hub genes exhibited stepwise changes across different groups,

indicating their potential as biomarkers for early CRC diagnosis and CRA monitoring. Vitamin D levels decrease from normal mucosa to CRC, implying that vitamin D-related genes may have synergistic roles in CRC development. Moreover, vitamin D intervention in CRC cell lines led to downregulation of MMP1 and CCND1 and upregulation of CEACAM1, SOSTDC1, and PRKAA2, suggesting that vitamin D may inhibit CRC through these genes.

In summary, this study underscores the significant role of vitamin D and its related genes along the NC-CRA-CRC continuum, offering valuable insights for preventive CRC treatment. Limitations include the need for more clinical samples and clarity on specific mechanisms. However, there are several limitations to the research. Firstly, additional clinical samples and multi-center studies are needed to further validate the differences in vitamin D concentrations and VDR SNPs across various CRCs. Verifying the hub genes and expanding the sample size to include different stages of CRC would strengthen the findings. Furthermore, the molecular functions of these hub genes in CRA remain unclear and require further investigation. Using shRNA targeting these genes could enhance the reliability of this study and will be a key focus for future studies.

Conclusion

This study is the first to perform a dynamic and systematic analysis of vitamin D levels and related genes across the NC-CRA-CRC continuum. It identified 5 hub genes—SOSTDC1, CCND1, CEACAM1, MMP1, and PRKAA2—as potential novel biomarkers for monitoring CRC. The study found that in vivo vitamin D intervention can regulate the expression of these hub genes, implicating its role in CRC development. However, further experimental validation is required to support these findings. Consequently, our study introduces innovative and reliable biomarkers for CRC, which could help predict adenoma malignancy and enhance the clinical application of CRA and CRC diagnosis, targeted therapy, and prognosis.

Abbreviations

CRC,Colorectal Cance; CRA,Colorectal Adenoma; Vitamin D receptor (VDR); SNPs, Single nucleotide polymorphisms;1,25$(OH)_2D_3$, 1,25-Dihydroxyvitamin D3; IHC, immunohistochemistry; KEGG, Kyoto Encyclopedia of Genes and Gnomes; OS, overall survival; RT-PCR, real-time polymerase chain reaction;GO, Gene Ontology; MMP1, Matrix metalloproteinase-1;CEACAM1,Carcinoembryonic Antigen-related Cell Adhesion Molecule 1;SOSTDC1, Sclerostin domain-containing protein-1;CCND1,cyclin D1;PRKAA2, protein kinase AMP-activated catalytic subunit alpha 2.

Ethics Approval

This study complies with the Declaration of Helsinki. This study was approved by the ethical committee of the Second Affiliated Hospital of Baotou Medical College. Ethics Approval Number:2023 ZX-008.

Author Contributions

All authors made a significant contribution to the work reported, whether that is in the conception, study design, execution, acquisition of data, analysis and interpretation, or in all these areas; took part in drafting, revising or critically reviewing the article; gave final approval of the version to be published; have agreed on the journal to which the article has been submitted; and agree to be accountable for all aspects of the work.

Funding

This work was supported by the Qin Wenbin Fund Project Plan, Qingmiao Plan of Baotou Medical College, Baotou Health Science and Technology Plan Project (Grant Numbers: BYJJ-QWB202213, BYJJ-ZRQM202230, wsjkkj2022055, and 2024wsjkkj59).

Disclosure

Lu Wang and Ruize Xu are co-first authors for this study. The authors have no relevant financial or non-financial interests to disclose for this work.

References

1. Sung H, Ferlay J, Siegel RL, et al. Global Cancer Statistics 2020: GLOBOCAN estimates of incidence and mortality worldwide for 36 cancers in 185 countries. *CA Cancer J Clin*. 2021;71(3):209–249. doi:10.3322/caac.21660
2. Xia C, Dong X, Li H, et al. Cancer statistics in China and United States, 2022: profiles, trends, and determinants. *Chin Med J*. 2022;135 (5):584–590. doi:10.1097/CM9.0000000000002108
3. Wang H, Cao MD, Liu CC, et al. [Disease burden of colorectal cancer in China: any changes in recent years?]. *Zhonghua Liu Xing Bing Xue Za Zhi*. 2020;41(10):1633–1642. Danish. doi:10.3760/cma.j.cn112338-20200306-00273
4. Ionescu VA, Gheorghe G, Bacalbasa N, Chiotoroiu AL, Diaconu C. Colorectal cancer: from risk factors to oncogenesis. *Medicina*. 2023;59 (9):1646. doi:10.3390/medicina59091646
5. Carlberg C. Vitamin D in the context of evolution. *Nutrients*. 2022;14(15):3018. doi:10.3390/nu14153018
6. Fleet JC, DeSmet M, Johnson R, Li Y. Vitamin D and cancer: a review of molecular mechanisms. *Biochem J*. 2012;441(1):61–76. doi:10.1042/BJ20110744
7. Abu El Maaty MA, Wölfl S. Effects of $1,25(OH)_2D_3$ on cancer cells and potential applications in combination with established and putative anti-cancer agents. *Nutrients*. 2017;9(1):87. doi:10.3390/nu9010087
8. Zhou A, Li L, Zhao G, et al. Vitamin D3 inhibits helicobacter pylori infection by activating the VitD3/VDR-CAMP pathway in mice. *Front Cell Infect Microbiol*. 2020;10:566730. doi:10.3389/fcimb.2020.566730
9. Feldman D, Krishnan AV, Swami S, Giovannucci E, Feldman BJ. The role of vitamin D in reducing cancer risk and progression. *Nat Rev Cancer*. 2014;14(5):342–357. doi:10.1038/nrc3691
10. Ferrer-Mayorga G, Gómez-López G, Barbáchano A, et al. Vitamin D receptor expression and associated gene signature in tumour stromal fibroblasts predict clinical outcome in colorectal cancer. *Gut*. 2017;66(8):1449–1462. doi:10.1136/gutjnl-2015-310977
11. Uitterlinden AG, Fang Y, Van Meurs JB, Pols HA, Van Leeuwen JP. Genetics and biology of vitamin D receptor polymorphisms. *Gene*. 2004;338 (2):143–156. doi:10.1016/j.gene.2004.05.014
12. Liu J, Lichtenberg T, Hoadley KA, et al. An integrated TCGA pan-cancer clinical data resource to drive high-quality survival outcome analytics. *Cell*. 2018;173(2):400–16.e11. doi:10.1016/j.cell.2018.02.052
13. Shen W, Song Z, Zhong X, et al. Sangerbox: a comprehensive, interaction-friendly clinical bioinformatics analysis platform. *iMeta*. 2022;1(3):e36. doi:10.1002/imt2.36
14. Barber LE, Bertrand KA, Petrick JL, et al. Predicted Vitamin D status and colorectal cancer incidence in the Black Women's Health Study. *Cancer Epidemiol Biomarkers Prev*. 2021;30(12):2334–2341. doi:10.1158/1055-9965.EPI-21-0675
15. Carlberg C, Velleuer E. Vitamin D and the risk for cancer: a molecular analysis. *Biochem Pharmacol*. 2022;196:114735. doi:10.1016/j.bcp.2021.114735
16. Ma Y, Zhang P, Wang F, Yang J, Liu Z, Qin H. Association between vitamin D and risk of colorectal cancer: a systematic review of prospective studies. *J Clin Oncol*. 2011;29(28):3775–3782. doi:10.1200/JCO.2011.35.7566
17. Carlberg C, Muñoz A. An update on vitamin D signaling and cancer. *Semin Cancer Biol*. 2022;79:217–230. doi:10.1016/j.semcancer.2020.05.018
18. Sun J, Zhang YG. Vitamin D receptor influences intestinal barriers in health and disease. *Cells*. 2022;11(7):1129. doi:10.3390/cells11071129
19. Gnagnarella P, Raimondi S, Aristarco V, et al. Vitamin D receptor polymorphisms and cancer. *Adv Exp Med Biol*. 2020;1268:53–114. doi:10.1007/978-3-030-46227-7_4
20. Al-Ghafari AB, Balamash KS, Al Doghaither HA. TaqI and ApaI Variants of Vitamin D receptor gene increase the risk of colorectal cancer in a Saudi population. *Saudi J Med Med Sci*. 2020;8(3):188–195. doi:10.4103/sjmms.sjmms_357_19
21. Wang G, Li BQ, Zhou HH. [Polymorphism of vitamin D receptor Fok I and colorectal cancer risk in Chinese]. *Zhong Nan Da Xue Xue Bao Yi Xue Ban*. 2008;33(5):399–403. Dutch
22. Pezeshkian Z, Nobili S, Peyravian N, et al. Insights into the role of matrix metalloproteinases in precancerous conditions and in colorectal cancer. *Cancers*. 2021;13(24):6226. doi:10.3390/cancers13246226
23. Amirkhizi F, Ghoreishy SM, Baker E, Hamedi-Shahraki S, Asghari S. The association of vitamin D status with oxidative stress biomarkers and matrix metalloproteinases in patients with knee osteoarthritis. *Front Nutr*. 2023;10:1101516. doi:10.3389/fnut.2023.1101516
24. Kim SH, Baek MS, Yoon DS, et al. Vitamin D inhibits expression and activity of matrix metalloproteinase in Human Lung Fibroblasts (HFL-1) Cells. *Tuberc Respir Dis*. 2014;77(2):73–80. doi:10.4046/trd.2014.77.2.73
25. Vara-Ciruelos D, Russell FM, Hardie DG. The strange case of AMPK and cancer: Dr Jekyll or Mr Hyde? (†). *Open Biol*. 2019;9(7):190099. doi:10.1098/rsob.190099
26. Ferreira GB, Vanherwegen AS, Eelen G, et al. Vitamin D3 induces tolerance in human dendritic cells by activation of intracellular metabolic pathways. *Cell Rep*. 2015;10(5):711–725. doi:10.1016/j.celrep.2015.01.013
27. Millan AJ, Elizaldi SR, Lee EM, et al. Sostdc1 regulates NK cell maturation and cytotoxicity. *J Immunol*. 2019;202(8):2296–2306. doi:10.4049/jimmunol.1801157
28. Tong X, Zhu C, Liu L, et al. Role of Sostdc1 in skeletal biology and cancer. *Front Physiol*. 2022;13:1029646. doi:10.3389/fphys.2022.1029646
29. Blish KR, Wang W, Willingham MC, et al. A human bone morphogenetic protein antagonist is down-regulated in renal cancer. *Mol Biol Cell*. 2008;19(2):457–464. doi:10.1091/mbc.e07-05-0433
30. Gopal G, Raja UM, Shirley S, Rajalekshmi KR, Rajkumar T. SOSTDC1 down-regulation of expression involves CpG methylation and is a potential prognostic marker in gastric cancer. *Cancer Genet*. 2013;206(5):174–182. doi:10.1016/j.cancergen.2013.04.005
31. Rawat A, Gopisetty G, Thangarajan R. E4BP4 is a repressor of epigenetically regulated SOSTDC1 expression in breast cancer cells. *Cell Oncol Dordr*. 2014;37(6):409–419. doi:10.1007/s13402-014-0204-6
32. Chang L, Guo R, Yuan Z, Shi H, Zhang D. LncRNA HOTAIR regulates CCND1 and CCND2 expression by sponging miR-206 in ovarian cancer. *Cell Physiol Biochem*. 2018;49(4):1289–1303. doi:10.1159/000493408
33. Orhan C, Bulut P, Dalay N, Ersen E, Buyru N. Downregulation of TCEAL7 expression induces CCND1 expression in non-small cell lung cancer. *Mol Biol Rep*. 2019;46(5):5251–5256. doi:10.1007/s11033-019-04982-6
34. Xie M, Zhao F, Zou X, Jin S, Xiong S. The association between CCND1 G870A polymorphism and colorectal cancer risk: a meta-analysis. *Medicine*. 2017;96(42):e8269. doi:10.1097/MD.0000000000008269
35. Ershov P, Poyarkov S, Konstantinova Y, Veselovsky E, Makarova A. Transcriptomic signatures in colorectal cancer progression. *Curr Mol Med*. 2023;23(3):239–249. doi:10.2174/1566524022666220427102048

36. Gray-Owen SD, Blumberg RS. CEACAM1: contact-dependent control of immunity. *Nat Rev Immunol*. 2006;6(6):433–446. doi:10.1038/nri1864
37. Yang L, Liu Y, Zhang B, et al. CEACAM1 is a prognostic biomarker and correlated with immune cell infiltration in clear cell renal cell carcinoma. *Dis Markers*. 2023;2023:3606362. doi:10.1155/2023/3606362
38. Yang C, Cao M, Liu Y, et al. Inhibition of cell invasion and migration by CEACAM1-4S in breast cancer. *Oncol Lett*. 2017;14(4):4758–4766. doi:10.3892/ol.2017.6791
39. Wegwitz F, Lenfert E, Gerstel D, et al. CEACAM1 controls the EMT switch in murine mammary carcinoma in vitro and in vivo. *Oncotarget*. 2016;7(39):63730–63746. doi:10.18632/oncotarget.11650